Microporous and Mesoporous Materials 243 (2017) 311–318

Contents lists available at ScienceDirect

Microporous and Mesoporous Materials

journal homepage: www.elsevier.com/locate/micromeso

Fabrication of hydrophobic composite films by sol-gel process between POSS -containing fluorinated polyacrylate latexes and colloidal silica particles

Xiangxuan Huang [a], Wenbo Liao [a, *], Lingyun Ye [a], Ni Zhang [a], Shanhong Lan [a], Hongbo Fan [a], Jinqing Qu [b]

[a] School of Chemistry and Environmental Engineering, Dong Guan University of Technology, Dongguan, 523808, China
[b] School of Chemistry and Chemical Engineering, South China University of Technology, Guangzhou, 510640, China

ARTICLE INFO

Article history:
Received 14 March 2016
Received in revised form
4 February 2017
Accepted 13 February 2017

Keywords:
Colloidal silica
POSS
Sol-gel process
Hydrophobicity

ABSTRACT

A novel hydrophobic composite films (POSS-FPA-SiO_2) were prepared by directly physically mixing octavinyl polyhedral oligomeric silsesquioxane containing fluorinated polyacrylate latexes (POSS-FPA) with colloidal silica. Sol-gel processes were carried out on the surface of POSS with addition of co-solvent to enhance roughness and hydrophobicity of composite films. TEM photos revealed that colloidal silica particles had enriched and aggregated on the surface of POSS, the sol-gel processes of silica particles occurred to form raspberry-like structure particles. The average diameter data indicated that the aggregation of colloidal silica particles on the surface of POSS had increased the average diameter of the composite latexes. FT-IR spectra confirmed that two kinds of –Si–O– bonds existed in the composite films, which one related to the Si–O framework of POSS and the other obtained form the sol-gel processes. SEM and AFM images illustrated that the coarse structure obtained from the sol-gel processes had increased the roughness of the composite surface. The water contact angle (WCA) of composite films were found increasing as the sol-gel processes. TGA curves demonstrated that the composite films exhibited much better thermal stability than that of pure FPA and POSS-FPA films.

1. Introduction

Hybrid materials with both inorganic and organic components draw more and more attentions because of its combination of the advantages of both inorganic materials and organic polymers [1,2]. Polyhedral oligomeric silsesquioxanes (POSS) is a class or organic-inorganic hybrid nanomaterial constituted by an inorganic silica $R_n(SiO_{1.5})_n$ core cage structure, where n (n = 8, 10, 12) is the number of silicon atoms of the cage and the R is a range of organic functional groups such as hydrogen, alkyl, alkene, aryl arylene groups, etc [3–5]. Those functional groups attached on POSS and make it easily to incorporate into polymer system via blending, grafting or copolymerization [6–11].

Many studies have reported about the preparation of POSS-based hybrid polymers with different architecture, such as dumbbell-type, pendent-type, bead-type, star-type or network-type, from atom transfer radical polymerization (ATRP), reversible addition-fragmentation chain transfer polymerization (RAFT), emulsion polymerization and so on [12–14]. The hybrid polymers display a number of desirable properties, especially the high thermal stability, high glass transition temperatures, flammability resistance, and hydrophobicity [11]. Usually, the incorporation of POSS units into polymer may improve the properties such as mechanical strength, hydrophobicity and thermal stability, and can also increase surface roughness [1,15]. However, the improvement of surface roughness and hydrophobicity was limited because of the small particle diameter sizes of POSS [16].

In our previous study, we have prepared polyacrylate/silica hybrid materials by directly mixing colloidal with KH570 modified polyacrylate emulsion, the sol-gel processes of colloidal silica particles were carried out by addition of co-solvent to form Si–O–Si crosslinking during film-formation [17,18]. We also had successfully synthesized octavinyl polyhedral oligomeric silsesquioxane grafted fluorinated polyacrylate (OvPOSS/FPSA) composite materials via emulsion polymerization, and it was found that the composite films

* Corresponding author.
E-mail address: liaowenbo110@163.com (W. Liao).

http://dx.doi.org/10.1016/j.micromeso.2017.02.045
1387-1811/

exhibited better thermal stability and hydrophobicity [19]. However, the maximum WCA of composite films only up to 102°, which indicated that the improvement of hydrophobicity of composite films was still limited. Therefore, in present paper, a novel hydrophobic composite films (POSS-FPA-SiO_2) were prepared by directly physical mixing octavinyl polyhedral oligomeric silsesquioxane containing fluorinated polyacrylate latexes (POSS-FPA) with colloidal silica, sol-gel processes of colloidal silica was induced with addition of co-solvent to built coarse structure in low surface energy surface during film-formation (Scheme 1). The morphology, chemical structures, average diameter sizes, surface morphology, hydrophobicity and thermal stability have been studied.

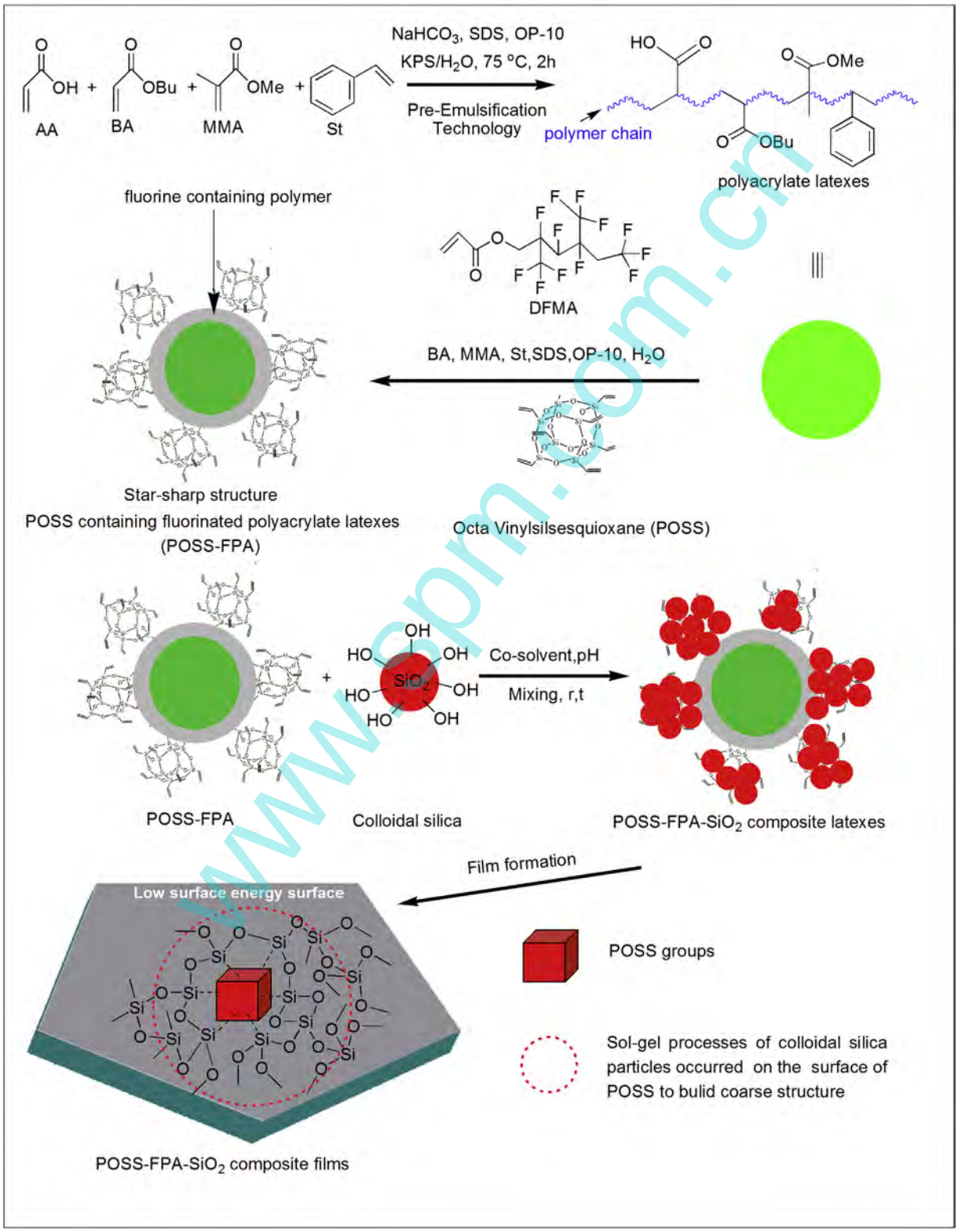

Scheme 1. The synthetic route of POSS-FPA-SiO_2 composite materials.

2. Experimental

2.1. Materials

The octavinyl polyhedral oligomeric silsesquioxane (POSS) was purchased from Baxi Equipment Co. (Changsha, China). Dodecafluoroheptyl methacrylate (DFMA) was purchased from Harbin Xuejia fluorin silicon Chemical Co. (Harbin, China). Methyl methacrylate (MMA) was supplied by Shanghai Lingfeng Chemical Co. (Shanghai, China). Butyl acrylate (BA), acrylic acid (AA), and styrene (St) were supplied by Tianjin Fuchen Co. (Tianjin, China) and used without further purification. Colloidal silica (30 wt%, pH = 11, the diameter size is about 20–50 nm) was supplied by Foshan Nanhai Waterglass Co. (Foshan, China). Ethanol were supplied by Guangzhou Chemical Reagent Co. (Guangzhou, China). Nonyl phenyl polyoxyethylene ether-10 (OP-10), sodium dodecyl sulphonate (SDS), sodium bicarbonate ($NaHCO_3$) and potassium persulfate (KPS) were used as received without further purification. Deionized water was used for the polymerization process.

2.2. Preparation of POSS-FPA materials

POSS-FPA latexes were synthesized by two-stage emulsion polymerization under the protection of nitrogen according to the literature [18]. First, the mixture of core monomers was added to the mixed emulsifier (OP-10/SDS) aqueous solution under a magnetic stirrer and pre-emulsified for 0.5 h. Deionized water, buffer agent $NaHCO_3$, initiator KPS were charged into a 500 mL four-neck flask with a machine stirring, and heated to 80–82 °C, then 25 g of core monomers was dropped into the system and processed for 20 min to prepare the seed latex, the rest core monomer and initiator KPS solution was added in 2 h with continuous stirring. The system was kept temperature at 80–82 °C for 0.5 h after finishing dropping core monomers, and the polyacrylate latexes were obtained. Second, the shell pre-emulsification monomers with DFMA and POSS was prepared and added to the system in 1 h, the initiator KPS solution was dropped throughout the process at a rate of 10–15 droplet/min. After fishing the monomers, the reactor temperature was increased to 85 °C and lasted reaction for 0.5 h. The obtained POSS-FPA latexes were filtered through a 200-mesh sieve, and the FPA latex was prepared from the same method without addition of POSS. The detail procedure in shown in Scheme 1 and Table 1.

The POSS-FPA films with thickness 5 μm on glass were prepared by spin coating process. The spin speed and time are 300 rpm and 18 s, respectively. The films were dried at 60 °C for 1 h [19].

2.3. Preparation of POSS-FPA-SiO_2 composite materials

The POSS-FPA-SiO_2 composite latexes were prepared by adding colloidal silica and ethanol as co-solvent to POSS-FPA latexes at room temperature, and stirred for 12 h, keeping the pH of system at about 8.0. The POSS-FPA-SiO_2 composite films were prepared from the same spin coating process.

2.4. Characterizations

Solid content of FPA and FPA-POSS latexes were determined by weight loss method. A known weight of latexes (m_1) was dropped into the dry watch glass (m_0), then heated at 120 °C until the constant weight (m_2) was obtained. The solid content was calculated by following equation:

$$\text{Solid content } (\%) = \frac{m_2 - m_0}{m_1} \times 100$$

The morphologies were directly observed by using a JEM-2100F transmission electron microscope (TEM) (JEOL Ltd., Japan) with an acceleration voltage of 200 kV. The samples were diluted with deionized water into 0.1 wt%, then blotted gently on the surface of carbon-coated copper grid, and dried at room temperature under atmospheric pressure.

The latexes particle size and its distribution were determined with a granularity analyzer (ZS Nano S) from Malvern Co. (England). The samples were diluted with deionized water into 0.5 wt% before texted.

Fourier transformed infrared spectroscopy (FT-IR) spectra of samples dispersed in dry KBr pellets were obtained by an Nicolet Avata360 FT-IR spectrometer in a spectral range 500–4000 cm^{-1}.

Scanning electron microscopy (SEM) measurements were conducted using a JEOL JSM-6701 system. Atomic force microscope (AFM) images were obtained using tapping mode at room temperature on a CSPM5500A of Being Nano-Instruments Ltd., Guangzhou, China. The samples were all obtained from spin coating process.

Water contact angle (WCA) measurements using ultrapure water was performed with a OCA15 contact angle goniometer (Dataphysics Co., Germany) according to the sessile drop technique. At least five independent measurements were carried out and the mean value was determined.

The thermal stability of dried composite films were determined by the Thermogravimetric analyzer (TG/DSC, STA449C) (Netzsch Co. Germany) by heating the sample (8–10 mg) from room temperature to 600 °C at 10 °C/min and at an air flow rate of 30 mL/min. In order to remove the water inside the films, the temperature would keep at 100 °C for 3 min. The TGA samples were prepared by the method described in the film preparation. The residual weight content was calculated by following Eq:

$$\text{Residual weigh } (\%) = \frac{W_2 \times S_2}{W_1 \times S_1 + W_2 \times S_2}$$

W_1 is the mass of the POSS-FPA, S_1 is the solid content of POSS-FPA, W_2 is the mass of the colloidal silica (10 wt% POSS-FPA), and S_2 is the solid content of colloidal silica.

Table 1
Detail polymerization recipes of PA, FPA, POSS-FPA and POSS-FPA-SiO_2 latexes.

Samples	MMA/g	BA/g	St/g	AA/g	DFMA/g	POSS/g	colloidal silica/g
PA[a]	25.5	24.5	18	2	0	0	0
FPA[b]	35.5	34.5	28	2	10	0	0
POSS-FPA	35.5	34.5	28	2	10	1	0
POSS-FPA-SiO_2[c]	35.5	34.5	28	2	10	1	10

[a] The weight ratio of core and shell monomer was 7/3.
[b] DFMA and POSS were dropped with the shell monomers.
[c] The weight ratio of colloidal silica and POSS-FPA latexes is 10%.

3. Results and discussion

3.1. The preparation of the POSS-FPA and POSS-FPA-SiO_2 composite materials

As reported in our previous study, vinyl-POSS is successfully grafted onto the surface of fluorinated polyacrylate latexes, and the synthesized latexes are mainly star-type structure, as shown in Fig. 1(a), due to the steric effect of POSS cage-like structures [10–14,19].

Since the POSS has a Si–O nanostructure inorganic framework and organic groups around the framework, which similar to that of colloidal silica. Furthermore, POSS cages also exhibit high specific surface areas and surface energy because of nanoscale, which make the surface atom of POSS in the highly activation station states [1,4]. When the POSS-FPA latexes blend with colloidal silica, the induced aggregation of silica particles on the surface of POSS occurs in order to maintain thermodynamic equilibrium [1,20]. It was assumed that sol-gel processes were carried out with addition of co-solvent during aggregation of silica particles and raspberry-like composite particles were obtained. Fig. 1(b) shows the TEM micrographs of the POSS-FPA-SiO_2 composite latexes. It can be observed that colloidal silica particles were aggregated on the surface of POSS rather than uniformly dispersed, and the sol-gel process of silica particles occurred during aggregation, leading to form raspberry-like structure particles.

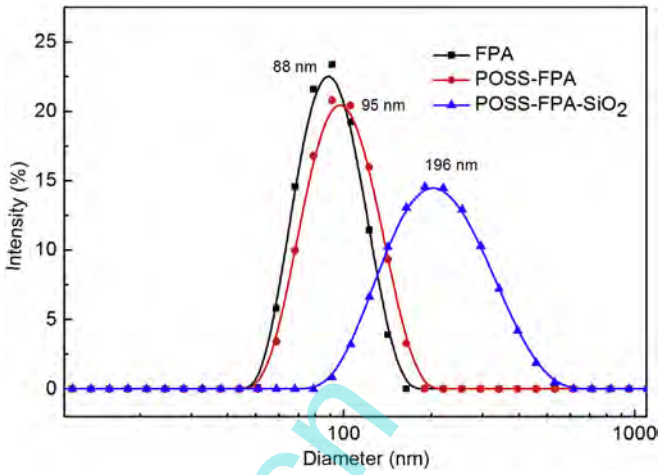

Fig. 2. The particle sizes and distributions of FPA latexes, POSS-FPA latexes and POSS-FPA-SiO_2 composite latexes.

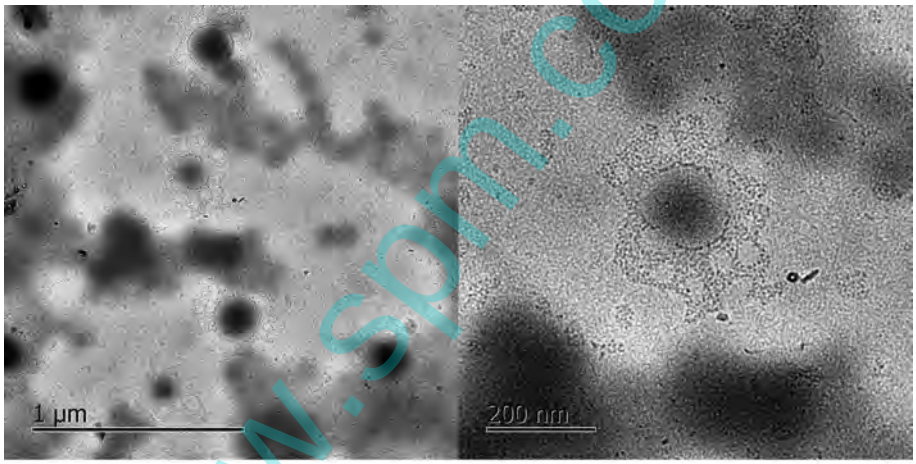

(a) POSS-FPA

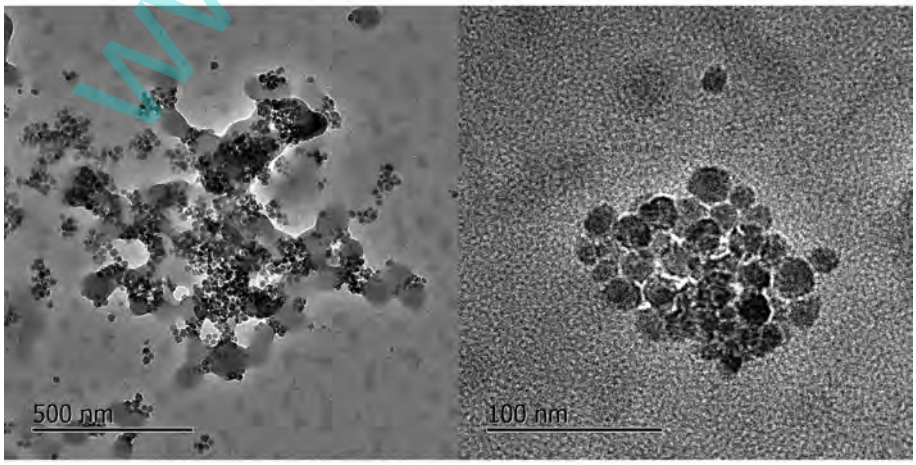

(b) POSS-FPA-SiO_2

Fig. 1. TEM photographs of POSS-FPA latexes (a) and POSS-FPA-SiO_2 composite latexes (b).

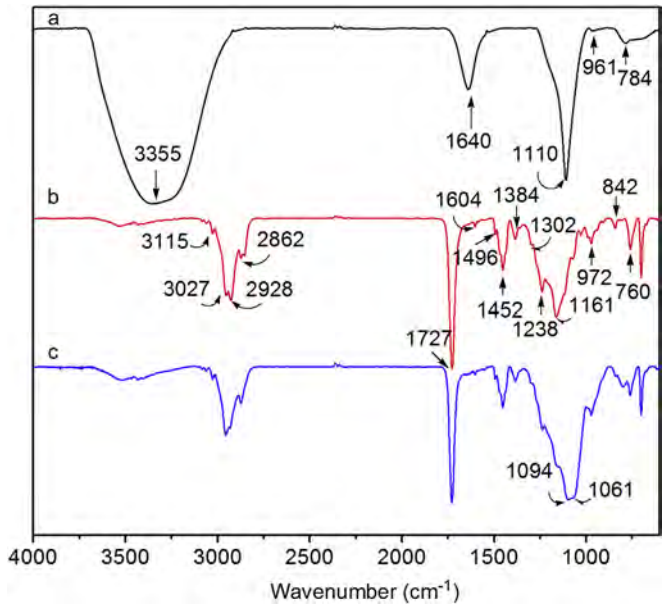

Fig. 3. FT-IR spectra of colloidal silica (a), POSS-FPA film (b) and POSS-FPA-SiO_2 composite film (c).

Fig. 2 illustrates the particle size distributions of the FPA, POSS-FPA latexes and POSS-FPA-SiO_2 composite latexes. The average diameter of FPA latexes is about 88 nm, while the diameter of POSS-FPA latexes is 95 nm, which is slightly bigger than that of the FPA. It was probability attribute to the encapsulation of POSS cages, which shown in Scheme 1. The average diameter of POSS-FPA-SiO_2 composite latexes increased to 196 nm, resulted from the aggregation of silica particles on the surface of POSS.

3.2. The chemical structure

Fig. 3 shows the FTIR spectra of colloidal silica, POSS-FPA and POSS-FPA-SiO_2 composite films. In Fig. 3(a), the absorption peaks around 3355 and 961 cm^{-1} are associated with the stretching vibrations of Si—OH group, while 1110 and 800 cm^{-1} are attributed to the stretching vibrations of Si—O—Si group, respectively [17]. In Fig. 3(b), The characteristic stretching peaks of $-CH_3$ and $-CH_2$ groups are at 2953 and 2862 cm^{-1}, respectively. The stretching vibration of C═O group at 1727 cm^{-1} is attributed to the carboxy of FPA, while the absorption peak at 1496 cm^{-1} is related to phenyl group. The typical absorption at 1302 cm^{-1} and 1238 cm^{-1} are assigned to the —CF and $-CF_3$ stretching vibration peaks, which provided evidence that DFMA is copolymerized with acrylate monomers, and fluorinated polyacrylate were obtained [21]. The absorption peaks at 3115, 3027, 1604 and 972 cm^{-1} are due to the characteristic peaks of C═C groups, and the stretching vibration of —Si—O— groups at 1161 cm^{-1} is attributed to the introduction of POSS cages. It can reasonably assumed that POSS had already successfully grafted onto the surface of FPA latexes, although only part of eight reactive C═C groups had carried out copolymerization because of the steric effect. However, compared with the spectrum of POSS-FPA, two absorption peaks at 1094 and 1061 cm^{-1} appeared at the same time in Fig. 3(c), the stretching vibration of Si—OH groups at 3355 and 961 cm^{-1} also disappeared. It can be possibly concluded that two kinds of —Si—O— bonds existed in the composite films, which one was related to the Si—O framework of POSS and the others came from the sol-gel processes of colloidal

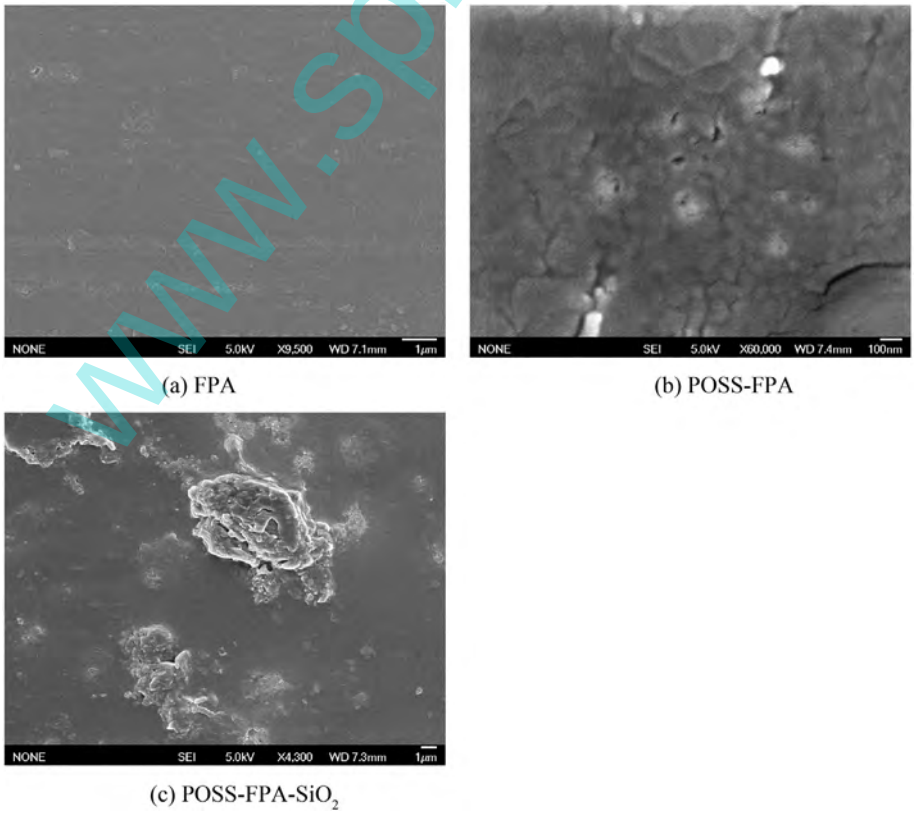

Fig. 4. SEM images of FPA film (a), POSS-FPA film (b), and POSS-FPA-SiO_2 composite film (c).

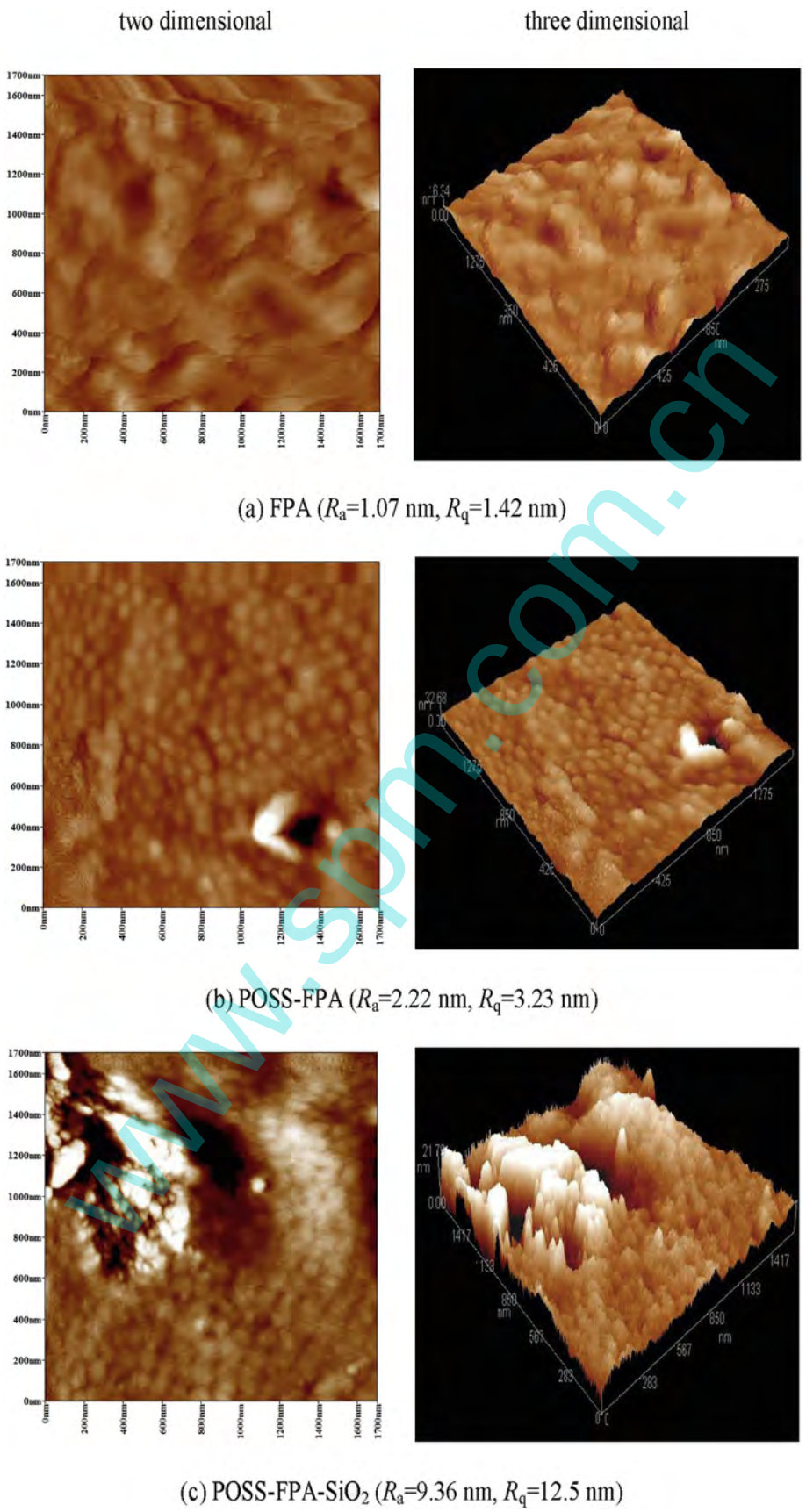

Fig. 5. AFM images of FPA film (a), POSS-FPA film (b) and POSS-FPA-SiO_2 composite film (c) with sizes of 17 μm × 17 μm.

silica particles. The FT-IR results provided further evidence that sol-gel processes of silica particles occurred during film-formation.

3.3. The surface morphology

The surface properties of composite film surface is affected by chemical composition and topography of composite surface [22]. The SEM, AFM and WCA measurements are used to examine the surface morphology of FPA, POSS-FPA films and POSS-FPA-SiO_2 composite films.

The SEM images of FPA, POSS-FPA films and POSS-FPA-SiO_2 composite films are displayed in Fig. 4. The FPA film had a smooth surface in Fig. 4(a), the surface of POSS-FPA film became rougher resulted from the grafting reaction, and many prominence were formed on the surface, as illustrated in Fig. 4(b). In Fig. 4(c), the aggregation of silica particles were found on some area of composite films, and the sol-gel processes occurred during film-formation to form raspberry-like structure particles.

The surface morphologies was also characterized by AFM. Surface topography and surface average roughness (R_a), root mean square roughness (R_q) of FPA, POSS-FPA films and POSS-FPA-SiO_2 composite films in an area of 1.7 μm × 1.7 μm were examined by atomic force microscope (AFM), as illustrated in Fig. 5. It was found that the surface of FPA film seems to be smooth. After grafting reaction, the POSS-FPA film surface became rougher, the R_a and R_q was increased from 1.07 to 1.42 nm to 2.22 and 3.23 nm, respectively, which confirmed that the grafting reaction had increased the roughness of composite surface. However, the R_a and R_q of POSS-FPA-SiO_2 composite films was increased to 9.36 and 12.5 nm, respectively, which was attributed to the sol-gel processes of silica particles on the surface of POSS to form coarse structure. Those results provided another evidence that sol-gel processes of silica particles occurred during film-formation.

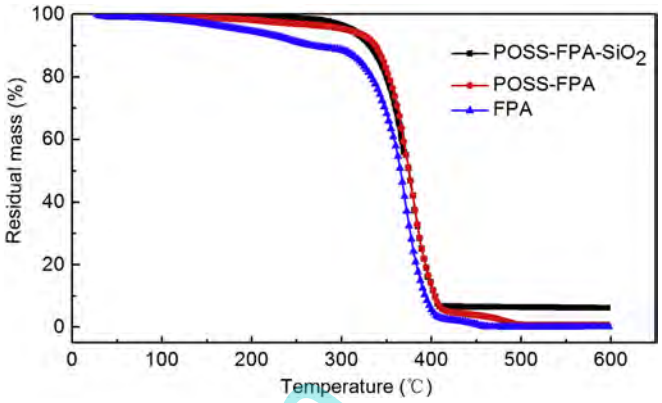

Fig. 7. TGA curves of FPA film (a), POSS-FPA film (b) and POSS-FPA-SiO_2 composite film (c).

The water contact angle (WCA) on film surface is dependent on surface elemental composite and structure, and films with a higher WCA generally display good hydrophobic and water-resistance [23,24]. To examine the hydrophobicity of the composite films surface, WCA measurements are carried out and shown in Fig. 6. It can be found that obvious changes of WCA were observed. In Fig. 6 (a), the WCA of FPA films is 61°, resulted form the copolymerization of hydrophilic monomer AA. The WCA increased to 102° while 1.0 wt% POSS was grafted onto the FPA latexes, as shown in Fig. 6 (b). POSS preferentially migrates toward the surface due to its low molecular weight and low surface energy by hydrophobic vinyl groups, resulting in making the surface much more hydrophobic [20]. In Fig. 6 (c), the WCA of POSS-FPA-SiO_2 composite films was up to 128°, which was attributed to the sol-gel process occurred to

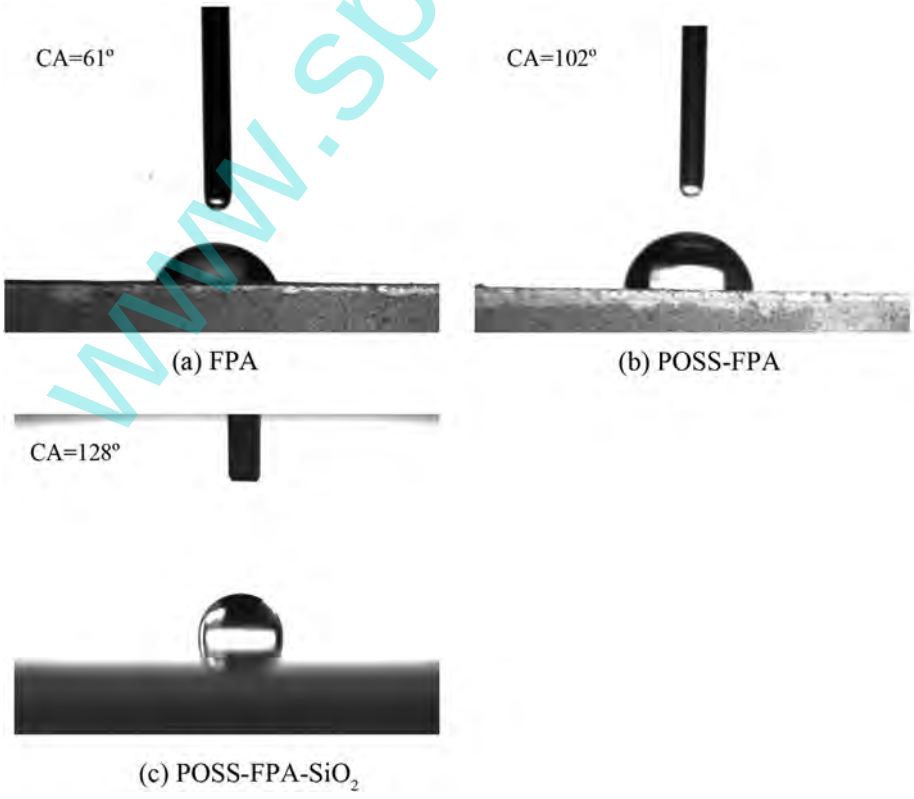

Fig. 6. WCA of FPA film (a), POSS-FPA film (b) and POSS-FPA-SiO_2 composite film (c).

form raspberry-like structure particles. Therefore, the POSS-FPA-SiO_2 composite films exhibited better hydrophobic than that of FPA and POSS-FPA films.

3.4. The thermal stability

The thermal decomposition behavior of FPA, POSS-FPA films and POSS-FPA-SiO_2 composite films were showed in Fig. 7. The temperature corresponding to 5 wt% loss was defined as the initial degradation temperature (T_d) [18]. The T_d of POSS-FPA films was 307 °C, which was about 120 °C higher than that of the FPA films. The result confirmed that the incorporation of POSS cages on the surface of FPA latexes had enhanced the thermal stability, and the increase of T_d was cause by the rigid nature of POSS cages which has the Si–O–Si framework and the steric effect may affect the movement of the local chain of the polymer. Sol-gel processes of silica particles occurred during POSS-FPA-SiO_2 composite film formation, and Si–O–Si crosslinking were obtained, which leading to the enhancement of the T_d. The T_d of POSS-FPA-SiO_2 composite film was increased to 315 °C, which displayed better thermal stability than that of FPA and POSS-FPA films. The residual weight of POSS-FPA-SiO_2 is 6.15%, while that of FPA and POSS-FPA is about 0.13% and 0.67%, indicating that the amount of inorganic compound related to POSS and SiO_2 is about 6.15%.

4. Conclusions

A novel hydrophobic composite films (POSS-FPA-SiO_2) were prepared by directly physically mixing octavinyl polyhedral oligomeric silsesquioxane containing fluorinated polyacrylate hybrid latexes (POSS-FPA) with colloidal silica. Sol-gel processes were carried out on the surface of POSS with addition of co-solvent to enhance roughness and hydrophobicity of composite films. TEM, SEM and AFM photos confirmed that colloidal silica particles had enriched and aggregated on the surface of POSS and sol-gel processes were carried out to increase the average diameter of composite latexes, roughness and hydrophobicity of the composite films surface. FT-IR spectra confirmed the sol-gel processes of colloidal silica particles had occurred. TGA curves demonstrated that the composite films exhibited much better thermal stability than that of FPA and POSS-FPA films.

Acknowledgements

We gratefully thank the “National Natural Science Foundation of China” (21446007) and “Natural Science Foundation of Guangdong Province, China” (2015A030310088) for financial support of this work.

References

[1] Y. Wang, F.G. Liu, X.X. Xue, Morphology and properties of UV-curing epoxy acrylate coating modified with methacryl-POSS, Prog. Org. Coatings 78 (2015) 404–410.
[2] G.X. Hou, J.G. Gao, C. Tian, X.J. Wu, Preparation and characterization of nanocomposite films by hybrid cationic ring opening polymerization of glycidyl-POSS, Mater. Chem. Phys. 148 (2014) 236–244.
[3] J.G. Gao, H.Q. Lv, X.F. Zhang, H.C. Zhao, Synthesis and properties of waterborne epoxy acrylate nanocomposite coating modified by MAP-POSS, Prog. Org. Coatings 76 (2013) 1477–1483.
[4] Q. Zhou, Z.Q. Wang, Y.L. Shi, J.H. Fang, H.Q. Gao, Leslie S. Loo, The migration of POSS molecules in PA6 matrix during phase inversion process, Appl. Surf. Sci. 284 (2013) 118–125.
[5] X. Qiang, X.Y. Ma, Z.G. Li, X.B. Hou, Synthesis of star-shaped polyhedral oligomeric silsesquioxane (POSS) fluorinated acrylates for hydrophobic honeycomb porous film application, Colloid Polym. Sci. 292 (2014) 1531–1544.
[6] H.Y. Xu, S.W. Kuo, C.F. Huang, F.C. Chang, Poly (acetoxystyrene-co-isobutylstyryl POSS) nanocomposites: characterization and molecular interaction, J. Polym. Res. 9 (2002) 239–244.
[7] K.W. Liang, H. Toghiani, Charles U. Pittman Jr., Synthesis, morphology and viscoelastic properties of epoxy/polyhedral oligomeric silsesquioxane (POSS) and epoxy/cyanate ester/POSS nanocomposites, J. Inorg. Organomet. Polym. Mater. 21 (2011) 128–142.
[8] O. Monticelli, A. Fina, A. Ullah, P. Waghmare, Preparation, characterization, and properties of Novel PSMA-POSS systems by reactive blending, Macromolecules 42 (2009) 6614–6623.
[9] E. Markovic, S. Clarke, J. Matisons, George P. Simon, Synthesis of POSS-methyl methacrylate-based cross-linked hybrid materials, Macromolecules 41 (2008) 1685–1692.
[10] B. Song, L.H. Meng, Y.D. Huang, Improvement of interfacial property between PBO fibers and epoxy resin by surface grafting of polyhedral oligomeric silsesquioxanes (POSS), Appl. Surf. Sci. 258 (2012) 10154–10159.
[11] F.Y. Ke, C. Zhang, S.Y. Guang, H.Y. Xu, POSS core star-shape molecular hybrid materials: effect of the chain length and POSS content on dielectric properties, J. Appl. Polym. Sci. 127 (2013) 2628–2634.
[12] Y.L. Ma, L. He, A.Z. Pan, C.B. Zhao, Poly (glycidyl methacrylate-POSS)-co-poly (methyl methacrylate) latex by epoxide opening reaction and emulsion polymerization, J. Mater. Sci. 50 (2015) 2158–2166.
[13] W.P. Wang, X.X. Jie, M. Fei, H. Jiang, Synthesis of core-shell particles by batch emulsion polymerization of styrene and octavinyl polyhedral oligomeric silsesquioxane, J. Polym. Res. 18 (2011) 13–17.
[14] B. Li, X.H. Li, K.Q. Zhang, H. Li, Y.H. Zhao, L.X. Ren, X.Y. Yuan, Synthesis of POSS-containing fluorosilicone block copolymers via RAFT polymerization for application ad non-wetting coating materials, Prog. Org. Coatings 78 (2015) 188–199.
[15] X.H. Li, K.Q. Zhang, Y.H. Zhao, K.Y. Zhu, X.Y. Yuan, Formation of icephobic film from POSS-containing fluorosilicone multi-block methacrylate copolymers, Prog. Org. Coatings 89 (2015) 150–159.
[16] H. Tang, T. Cao, X. Liang, A.F. Wang, O.S. Salley, J. Mcallister II, K.Y. Simon Ng, Influence of silicone surface roughness and hydrophobicity on adhesion and colonization of *Staphylococcus* epidermidis, J. Biomed. Mater. Res. Part A 88 (2009) 454–463.
[17] W.B. Liao, J.Q. Qu, Z. Li, H.Q. Chen, Preparation of organic/inorganic hybrid polymer emulsions with high silicon content and sol-gel-derived thin films, Chin. J. Chem. Eng. 18 (2010) 156–163.
[18] W.B. Liao, H.P. Teng, J.Q. Qu, T. Masuda, Fabrication of chemically bonded polyacrylate/silica hybrid films with high silicon contents by the sol-gel method, Prog. Org. Coatings 71 (2011) 376–383.
[19] W.B. Liao, X.X. Huan, L.Y. Ye, S.H. Lan, H.B. Fan, Synthesis of composite latexes of polyhedral oligomeric silsesquioxane and fluorine containing poly(styrene-acrylate) by emulsion copolymerization, J. Appl. Polym. Sci. 133 (2016), http://dx.doi.org/10.1002/APP.43455.
[20] E.H. Kim, S.W. Myoung, Y.G. Jung, U. Paik, Polyhedral oligomeric silsesquioxane-reinforced polyurethane acrylate, Prog. Org. Coatings 64 (2009) 205–209.
[21] K. Li, X.R. Zeng, H.Q. Li, X.J. Lai, Fabrication and characterization of stable superhydrophobic fluorinated-polyacrylate/silica hybrid coating, Appl. Surf. Sci. 298 (2014) 214–220.
[22] D.X. Han, L.Q. Zhu, Y.C. Chen, W.P. Li, L.L. Feng, Synthesis and characterization of acrylic latex: Effects of fluorine and silicon components on properties of the latex copolymers, J. Fluor. Chem. 156 (2013) 38–44.
[23] A.L. Qu, X.F. Wen, P.H. Pi, J. Cheng, Z.R. Yang, Gradient distribution of fluorine on the film surface of the organic–inorganic hybrid fluoropolymer, Colloids Surfaces A Physicochem. Eng. Aspects 345 (2009) 18–25.
[24] J.W. Fan, D.D. Li, W. Teng, J.P. Yang, Y. Liu, L.L. Liu, A.A. Elzatahry, A. Alghamdi, Y.H. Deng, G.M. Li, W.X. Zhang, D.Y. Zhao, Ordered mesoporous silica/polyvinylidene fluoride composite membranes for effective removal of water contaminants, J. Mater. Chem. A 4 (2016), 3859–3857.